



# Optimizing Regional Climate Model Output for Hydro-Climate Applications in the Eastern Nile Basin

Mahmoud Osman<sup>1,3</sup> · George Zittis<sup>2</sup> · Mohammed Haggag<sup>3</sup> · Ahmad W. Abdeldayem<sup>3</sup> · Jos Lelieveld<sup>2,4</sup>

Received: 5 March 2021 / Revised: 24 April 2021 / Accepted: 25 April 2021 / Published online: 5 May 2021  
© King Abdulaziz University and Springer Nature Switzerland AG 2021

## Abstract

This study focuses on the Eastern Nile (EN) Basin, most of whose water flows into the High Aswan Dam (HAD), Egypt. It is, therefore, crucial to have an accurate hydrological assessment overtime to plan water resource management in the area. With complex topography, it is important to capture most of the physics captured with the least bias in meteorological information. Weather Research and Forecasting (WRF) model was configured for a nested domain centered over the EN basin with a parent domain defined over the larger Middle East–North Africa (MENA) region at 0.09 degrees and 0.44 degrees spatial resolution, respectively. The bias correction of the model is performed with associated meteorological parameters. WRF physics parameterization sensitivity experiments were carried out to select an optimum combination of physics schemes. The model skill was also examined by downscaling the ERA-Interim reanalysis dataset from 1980 to 2009 over the EN basin domain. The WRF performance was assessed using gridded observational datasets for precipitation and temperature output. The results revealed significant positive precipitation bias, especially over the highlands. The bias-corrected precipitation data is coupled to the semi-distributed hydrological rainfall-runoff—Soil and Water Assessment Tool (SWAT)—model, previously configured for the Baro-Akobo-Sobat sub-basin. The simulated flow hydrograph based on bias-corrected WRF simulations enhanced high correlations and Nash–Sutcliffe Efficiency coefficients (from 0.61 to 0.79) for the observed flow hydrographs, hence improved hydrologic simulations. Results indicated that the bias-corrected precipitation fields from WRF can contribute to improved hydrological impact assessments.

**Keywords** Dynamic downscaling · Eastern Nile Basin · WRF · Hydroclimate applications

---

This study contributes to the development of an integrated hydro-climate model for the EN basin for the impact assessment of the Nile inflow at Aswan by configuring a RCM using WRF to downscale ERA-Interim reanalysis data from 1980 to 2009 and correct the resulting model bias.

---

✉ Mahmoud Osman  
mahosman01@gmail.com

<sup>1</sup> Earth and Planetary Sciences, Johns Hopkins University, Maryland, USA

<sup>2</sup> Climate and Atmosphere Research Center (CARE-C), The Cyprus Institute, Nicosia, Cyprus

<sup>3</sup> Irrigation and Hydraulics Department, Cairo University, Cairo, Egypt

<sup>4</sup> Department of Atmospheric Chemistry, Max Planck Institute for Chemistry, Mainz, Germany

## 1 Introduction

Global and regional climate models are being developed and widely used to project future climate conditions, and to help better understand the present and past climate (Buontempo et al. 2015; Clarke et al. 2007; Kalognomou et al. 2013; Lelieveld et al. 2012). Dynamic downscaling techniques can be applied to bring global-scale projections down to a regional level, where the output of general circulation models (GCMs) provides the initial and lateral boundary conditions, unlike statistical downscaling which develops statistical relationships between climate parameters, usually by a method of generating a modified local time series by translating a pattern into a local information (Giorgi 1990; Schmidli et al. 2007). Considerable computing resources are involved in dynamic downscaling, where high-resolution climate scenarios provided by regional climate models (RCMs) allow for a more precise description of topographic forcing due to orography, land-sea contrasts and land-use

characteristics (Cohen 1990; Evans 2012; Giorgi 1990). These complex feedbacks and processes are of particular relevance for the Eastern Nile (EN) Basin, where despite the projected warming, future precipitation changes are characterized by low levels of robustness (Lelieveld et al. 2016; Zittis et al. 2019). Moreover, parts of the Basin (mainly downstream) are expected to become drier, while regions upstream will likely become wetter (Almazroui et al. 2020; Driouech et al. 2020). Regional hydro-climate assessments for the future are still limited, and the level of understanding of future climate behavior is still developing for different sectors in the EN due to the cost and complexity of carrying out representative climate studies. The complexity and chaotic nature of the climate system and the synergetic effect of temperature and precipitation changes suggest that future hydroclimate conditions cannot be represented by extrapolating past climate conditions (Collins et al. 2013; Baumberger et al. 2017). Instead, the best prospects for predicting future behavior are using mathematical representations of the Earth's climate system through high-resolution regional climate and hydrological models that consider the peculiarities of the region. Although such applications are common in other parts of the world (Camera et al. 2020 and references therein), there is a lack of relevant research studies that assess the performance of the hydro-climate models over the Nile and specifically over the EN basin. Few studies (Argent, 2014; Beyene et al. 2010; Di Baldassarre et al. 2011; Siam 2010; Weldemariam 2015) focused on the impacts of climate change on the hydrology at different regions in the Nile basin hydrology and Lake Victoria basin using dynamical and statistical downscaling techniques.

In this context, this study pursues a high-resolution Regional Climate Model (RCM) configuration for the EN basin that is optimized and subsequently bias-corrected,

thus serving for hydro-climatological applications. Our Weather Research and Forecasting (WRF) model optimization involves the testing of several parameterization options of sub-grid scale processes (e.g., microphysics and planetary boundary layer), as well as the off-line coupling with a semi-distributed hydrological rainfall-runoff model, using the Soil and Water Assessment Tool (SWAT) model. The results of the study are expected to be used in future dynamic downscaling of climate models for hydro-climatological applications using the pre-configured WRF model.

## 2 Data and Methods

### 2.1 Study Region

The EN hydrologic boundaries extend from the Ethiopian Highlands ( $\sim 3^\circ$  N) in the south to the High Aswan Dam (HAD) in the North ( $\sim 24^\circ$  N) and from the west of Sudan ( $\sim 26^\circ$  E) to the Gulf of Aden ( $\sim 42^\circ$  E) as shown in Fig. 1. Elevations in the EN basin range from 0 to 4300 m above mean sea level. About 5% of the basin lies in very low elevated areas while most of the EN (around 70%) is situated within the range of 300–600 m. Another 20% is between 600–2000 m and the remaining 5% is associated with very steep slopes (around 2000–4300 m) (Tesemma 2009). Ethiopia has a general elevation ranging from 1500 to 3000 m and the plateau height exceeds 4000 m. A key land feature in Ethiopia is Lake Tana, created by volcanic activity, at a height of 1785 m. In Sudan, elevations vary between 170 m and 1475 m, whereas in South Sudan, elevation ranges from 380 to 2885 m (Asore 2012; Raafat 2015; Siam 2010; Tarabia 2015).

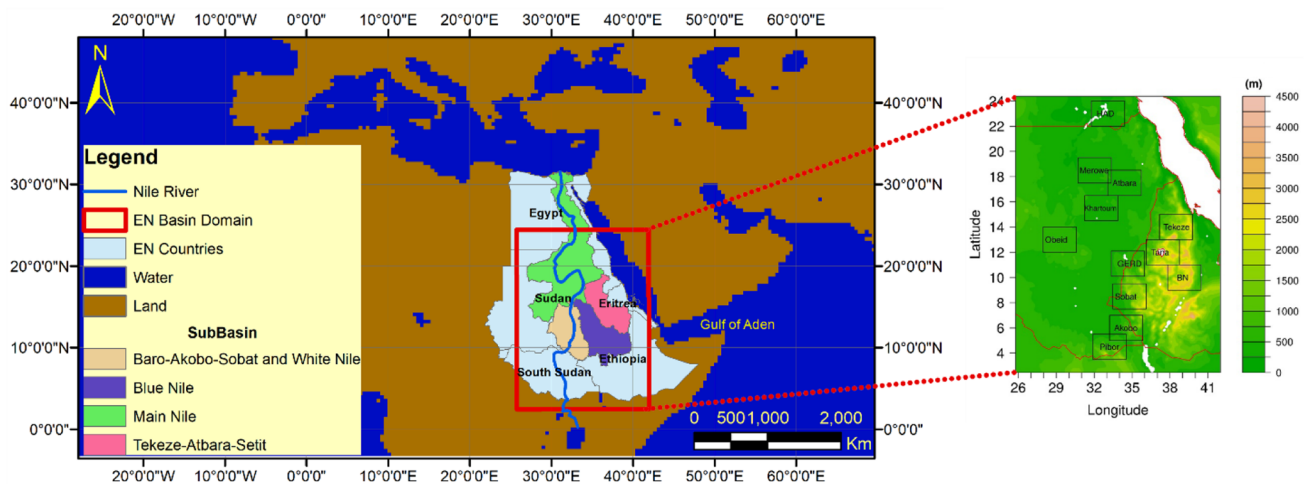


**Fig. 1** Region of a study showing the configured WRF EN basin domain nested in the MENA domain and the selected sub-regions for evaluation

The EN is divided into five sub-basins that include the Main Nile, the Baro-Akobo-Sobat,-White Nile, the Abay-Blue Nile, and the Tekeze-Atbara-Setite as shown in Fig. 1. The Abay-Blue Nile and the Main Nile region host nearly 82% of the total population (ENTRO 2006; Siam 2010). The EN basin region experience a tropical to subtropical climate with seasonally summer (June–August) precipitation that mostly happens in the south in Ethiopia and South Sudan. Precipitation over the Nile basin increases from the north to the south (with elevation) with values up to 1600 mm/year over the Ethiopian highlands, which is mainly governed by the interaction with the basin topography and the Inter-Tropical Convergence Zone movement (Mohamed et al. 2005; Tarabia 2015). Temperatures varies widely from a Mediterranean climate in the north (Lower Egypt) to cold over the Ethiopian plateau and hot in the central and northern Sudan. The average for the minimum temperature varies from 12 to 20 °C, while the average for maximum temperature varies from 29 to 33 °C.

Due to the varying climate conditions across the EN basin, a wide swath of landcover is observed. Most of the northern basin area are arid to semi-arid lands due to the dry climatic conditions, while the south near Ethiopia and South Sudan are greener lands, either cultivated or natural forests. The observed landcover over a period of nearly 50 years from 1961 to 2009 has changed a little; where the natural vegetation has decreased by nearly 1.8% and the agriculture area has increased by 5.3% resulting in a loss of 0.3 Mha of green areas (ENTRO 2006; Siam 2010; Tarabia 2015).

## 2.2 Datasets

Based on availability throughout the study period (1980–2009), spatial resolution and quality of data, the following sets are selected:

- European Centre for Medium-Range Weather Forecast (ECMWF) ERA-Interim reanalysis dataset. The ERA-Interim project started in 2006 to improve the ECMWF ERA-40 data (1957–2002) to introduce a better representation of the hydrological cycle, the quality of the stratospheric circulation, and the handling of biases and changes in the observing. The ERA-Interim atmospheric model and reanalysis system is coupled to an ocean-wave model and it is configured for 60 vertical atmospheric levels, with top level at 0.1 hPa system at approximately 80 km spatial resolution (Berrisford et al. 2011).
- The Global Precipitation Climatology Center (GPCC) dataset version 6.0, covering the period 1901–2010, contains monthly precipitation sums and has a spatial resolution of  $0.5^\circ \times 0.5^\circ$  latitude by longitude. GPCC is derived from archived and collected global precipitation data based on quality-controlled data from 67,200 sta-

tions for record durations of more than 10 years (Schamm et al. 2014). The GPCC dataset is selected for its appropriate resolution and quality for use of multiple regions over Africa (Nicholson et al. 2003; Zittis 2018).

- The University of Delaware (UDEL) monthly global dataset for air temperature and precipitation from 1950 to 2010 with a spatial resolution of  $0.5^\circ \times 0.5^\circ$  latitude by longitude (UDEL 2015).

## 2.3 Methods

The methodology applied for hydro-climatic simulations and dynamical climate downscaling over the EN basin is summarized in the flow chart of Fig. 2. The regional climate modeling is carried out using version 3.5 of the WRF model, developed at the National Center for Atmospheric Research (NCAR) (Skamarock et al. 2008), over a domain covering the Middle East and North Africa (MENA) including the EN region. This is defined by the MENA initiative of the Coordinated Regional Climate Downscaling Experiment—CORDEX (Zittis et al. 2014). Climate downscaling is performed by forcing the WRF model with initial and boundary conditions from the European Centre for Medium-Range Weather Forecast (ECMWF) ERA-Interim reanalysis dataset (Berrisford et al. 2011) for a 30-years period from 1980 to 2009, to (a) select the suitable combination of physics parameterizations and (b) investigate the model skill in reproducing the past and present climate conditions. The model is configured as a sub-domain (nest) in the MENA-CORDEX domain, encompassing  $185 \times 250$  horizontal grid points ( $\sim 10$  km grid resolution) and 30 vertical grid levels. The integration timestep is set to 240 s for the MENA parent domain computations and 1:5 as parent to nest timestep ratio which is the same ratio used for nesting the EN domain. The model is configured using the 21-categories MODIS satellite landcover dataset, with the default static datasets for soil, albedo, vegetation and topography (Skamarock et al. 2008). The spin-up time is set to seven months after sensitivity analysis to model for different spin-up periods.

Because the MENA-CORDEX domain is large and parts of it are out of context for the EN region, we focus our evaluation on the high-resolution nest and the 12 sub-domains listed in Table 1, that represent the individual watersheds of the EN and cover different climatic zones up to the High Aswan Dam. The selected regions are equally sized as boxes of dimensions  $2^\circ$  by  $2^\circ$  represented in Fig. 1. Each of them covers approximately 484 grid points at the EN domain selected resolution ( $\sim 10$  km grid resolution).

### 2.3.1 Sensitivity to Physics Parameterization

Based on previous WRF studies for the MENA-CORDEX domain (Abdelwares et al. 2017; Zittis et al. 2014, 2017)

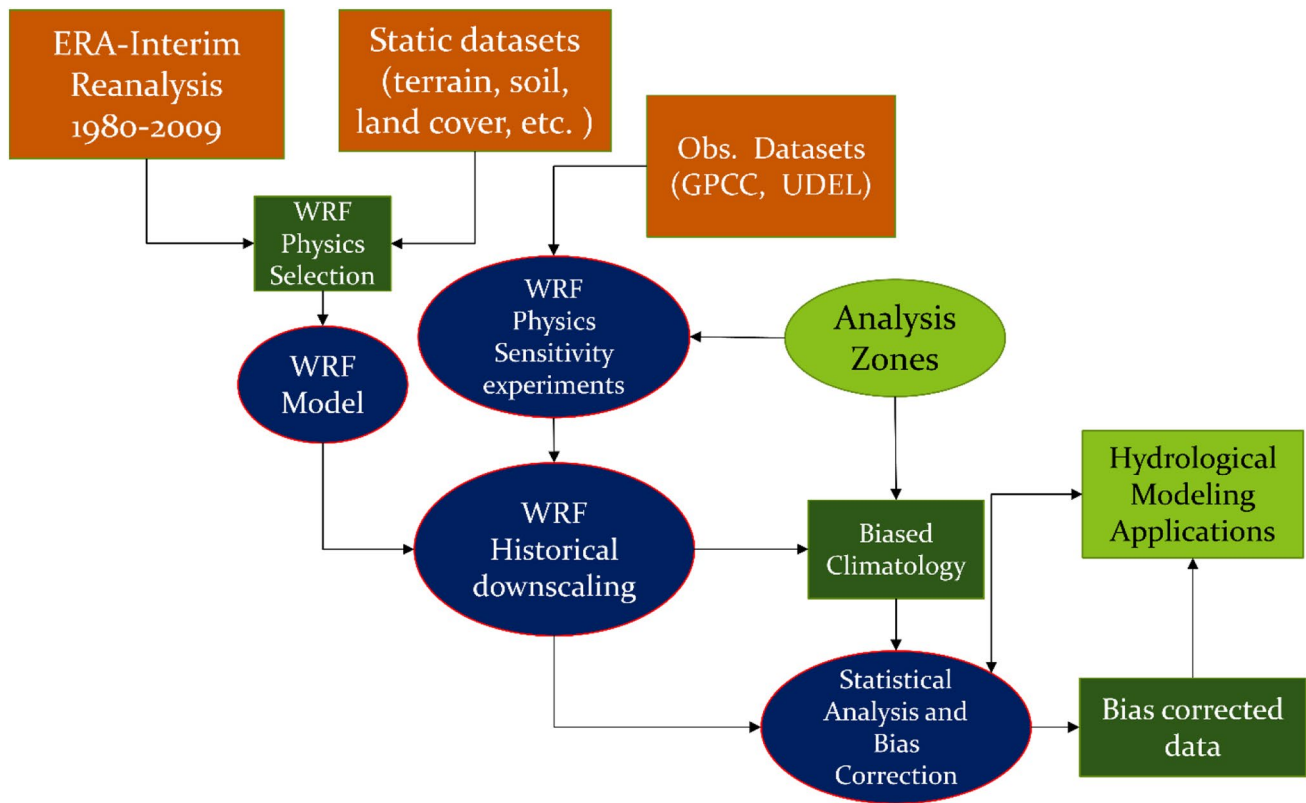


**Fig. 2** The followed research methodology flow chart

**Table 1** Names and locations of the 12 sub-regions for analysis

#	Name	Longitude (Degrees East)	Latitude (Degrees North)	Region
1	Tana	37.2	12.0	Lake Tana
2	GERD	34.8	11.1	Grand Ethiopian Renaissance Dam
3	HAD	32.9	23.0	High Aswan Dam
4	Khartoum	32.5	15.5	Khartoum
5	Atbara	34.4	17.5	Atbara River
6	Sobat	34.5	8.5	Sobat River
7	Merowe	32.0	18.5	Merowe Dam
8	Tekeze	38.0	14.0	Tekeze
9	Akobo	34.0	6.0	Akobo River
10	BN	39.0	10.0	Blue Nile River
11	Pibor	33.2	4.5	Pibor
12	Obeid	29.0	13.0	Obeid

and following other physics sensitivity studies (Caldwell et al. 2009; Done et al. 2005; Fujino et al. 2006; Gbobatiyi et al. 2014; Jin et al. 2010; Katragkou et al. 2015; Laprise et al. 2013; Otkin et al. 2006; Shin and Hong, 2011; Soares et al. 2012), four physics combinations, commonly used

**Table 2** WRF physics parameterization options tested in model sensitivity analyses

Physics	PH01	PH02	PH03	PH04
Microphysics	WSM6	Thompson	WSM6	LIN
Planetary Boundary Layer	MYJ	MYJ	YSU	MYJ

All other physics options are kept the same in the four experiments

for regional climate simulations, are used to test the model sensitivity towards different parameterization schemes (Table 2). In this task, we mainly focus on the microphysics and planetary boundary layer (PBL) parameterizations. The physics representations were tested for precipitation and temperature over 2 years of extreme different precipitation regimes over the Nile basin; 1999 as a wet year and 1984 as a dry year (Siam 2010).

As reference data for the model evaluation, we use the Global Precipitation Climatology Center (GPCC) dataset (Schamm et al. 2014) for precipitation, while the UDEL (UDEL 2015) provided the reference for temperature. The Pearson's correlation coefficient (COR) is used to determine the skill of the model to simulate the variables' pattern across the simulation period (Eq. 1). The Root Mean Square

Error (RMSE), (Eq. 2) and the Mean Absolute Error (MAE), (Eq. 3) are also calculated to assess the quality of the model and estimate model simulation biases:

$$COR = \frac{cov(OBS, SIM)}{\sigma_{OBS} \cdot \sigma_{SIM}} = \frac{\sum_{i=1}^n (OBS_i - \bar{OBS})(SIM_i - \bar{SIM})}{\sigma_{OBS} \cdot \sigma_{SIM}} \quad (1)$$

$$MAE = \frac{1}{n} \sum_{i=1}^n |SIM_i - OBS_i| \quad (2)$$

$$RMSE = \sqrt{\frac{\sum_{i=1}^n (SIM_i - OBS_i)^2}{n}} \quad (3)$$

Where  $n$  is the number of samples, and OBS and SIM are the observed and simulated variables.

The used observational datasets are bilinearly re-gridded to match the configured WRF model resolution, to carry out grid-to-grid statistical analysis.

### 2.3.2 Precipitation Bias Correction

Several bias correction methods have been proposed, focusing mainly on precipitation and temperature. In view of the intricacy of physical processes to simulate precipitation, there are different methods at different levels of complexity available, from simple linear methods to empirical or theoretical functions aiming to correct moments of precipitation distribution (Argüeso et al. 2013).

Following a wide variety of bias correction methods (Argüeso et al. 2013), the algorithm followed to correct the precipitation output of our climate simulations is based on verifying the adjusted rainfall rates by applying them to a semi-distributed Rainfall-Runoff hydrological model (SWAT) and assessing the quality of the output flow hydrograph compared to that observed. The aim is to ensure the adequacy of the corrected precipitation results for hydrologic applications. The SWAT model have been previously used in different studies for simulating streamflow and watershed modeling (Arnold and Fohrer 2005; Mengistu and Sorteberg 2012), due to its capabilities of simulating hydrological processes as well as land-management and agricultural scenarios to support water resources management under different scenarios (Arnold and Fohrer 2005).

The selected study region for the SWAT model is the Gambella watershed, which is a part of the Baro-Akobo-Sobat Sub-Basin of the EN as shown in Fig. 3. The Gambella watershed covers an area of approximately 23,450 km<sup>2</sup> over a wide elevation range, i.e. from a minimum of 450 m to a maximum of 2650 m. Raafat (2015) calibrated The SWAT model for Gambella watershed using ground-based observations of the runoff available near the streams following recommendations and sensitivity analysis of streamflow

under different climate change scenarios within the EN basin (Mengistu and Sorteberg 2012). In that study, the weather information used is pulled from the Global Historical Climatology Network (GHCN) dataset version 2. After calibration, the model has shown a very high coefficient of determination ( $R^2$ ) value of nearly 0.95, and a Nash–Sutcliffe Efficiency value (NSE) of 0.92.

The first bias-correction method is based on the probability distribution of the average monthly precipitation simulated from the WRF model in the whole domain (Legates and McCabe 1999). The modelled and observed precipitation (from GPCC dataset) fields are fitted and corrected according to a probability distribution function. The second correction method relies on inspection of the average precipitation bias over the experiment period against the elevation in each grid-point, then multiple bias correction factors are applied to the modelled precipitation based on the GPCC dataset to each topographic elevation group. The third bias correction method is based on evaluating the bias between the validation dataset and the monthly interannual variability in precipitation. The algorithm of correction depends on the daily average bias relative to the GPCC data in the same month, across the year for each grid-point in the domain. The three bias correction methods are evaluated based on the Nash–Sutcliffe Efficiency (NSE) of the SWAT model in using the corrected precipitation fields as the input for simulating the Gambella watershed runoff.

## 3 Results and Discussion

We performed a Taylor diagram-based statistical analysis for the four model configurations by comparing them with the UDEL dataset for the monthly average temperature in the historically wet year (1999) and dry year (1984). The analysis shows no significant difference between the chosen physics packages, which indicates that the four parameterization groups behave similarly in simulating the temperature over the Eastern Nile Basin (Fig. 4a). Physics configurations “1” and “4” show nearly similar performance for both precipitation and temperature for the selected 2 years (Fig. 4b). However, as an overall equally-weighted average for the RMSE and COR parameters for the selected 12 regions in the years 1984 and 1999, the performance of physics configuration “4” was found to give slightly better results (Table 3) and is selected for the historical 30 years downscaling experiment and includes “Lin” (Chen and Sun 2002) Microphysics scheme, “MYJ” (Janjić 1990) Planetary boundary layer parameterization scheme, “BMJ” Cumulus scheme (Janjić 1994), “CAM” (Collins et al. 2006) radiation scheme and “NOAH” (Chen et al. 1996) land surface model.

Precipitation results from WRF are still highly uncertain due to the complexity of cloud formation and the

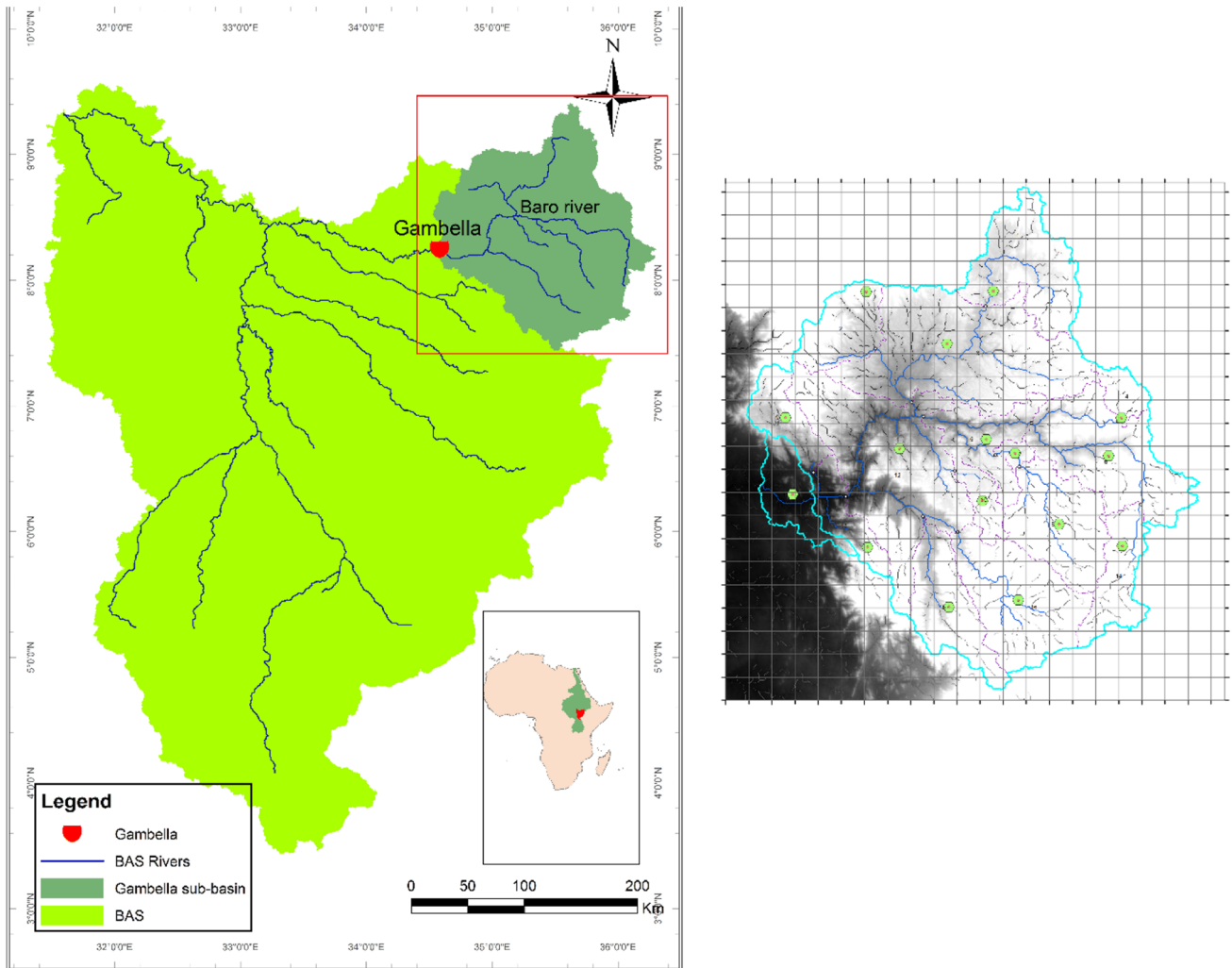


**Fig. 3** Left: Gambella watershed location within the Baro-Akobo-Sobat sub-basin. Right: a map of Gambella watershed within the WRF model grid at a resolution of  $0.09^{\circ} \times 0.09^{\circ}$ . “Light green circles with red dots” represent the used meteorological stations for the SWAT model configuration

precipitation physics representation. The model appears to overestimate precipitation over the highlands and underestimates it in low elevation regions, which needs further validation for application in hydrologic applications. Figure 5 shows the bias of the daily average over the 30-year period from 1980 to 2009.

The bias in precipitation is evident in the comparison for sub-regions, showing an underestimation in most of the dry parts and overestimation in the highlands, while both overestimation and underestimation were noticed in some regions like in Obeid. Figure 6 illustrates the modeled precipitation over three regions (Akobo, BN and GERD) out of the 12-selected analysis zones as time series of monthly precipitation (figures for other regions are not shown), averaged over all grid points of each sub-region. Interestingly, substantial differences between the monthly precipitations of the two gridded observational datasets

are also found. These underscore concerns regarding the uncertainty in observational datasets (Tanarhte et al. 2012; Zittis 2018).

The modeled precipitation is still subject to bias correction due to the obvious bias in modeling the past/present compared to the GPCC and UDEL datasets. The following sections will discuss in detail the correction methods followed, and the hydrologic verification technique to assure the adequacy of the chosen correction method (Elshamy et al. 2009).

According to the proposed first bias-correction method, the monthly GPCC precipitation is found to be best fitted as Weibull distribution with a maximum likelihood method, and shape and scale factors equal to 1.279 and 1.545, respectively, as shown in Fig. 7a, while the modeled precipitation has shape and scale factors equal to 1.202 and 1.183, respectively, as shown in Fig. 7b.

**Fig. 4** **a** Taylor diagram for temperature over the EN basin for the four physics groups over the two test years, 1984 and 1999. **b** Similar to **a** for the total precipitation over the EN basin

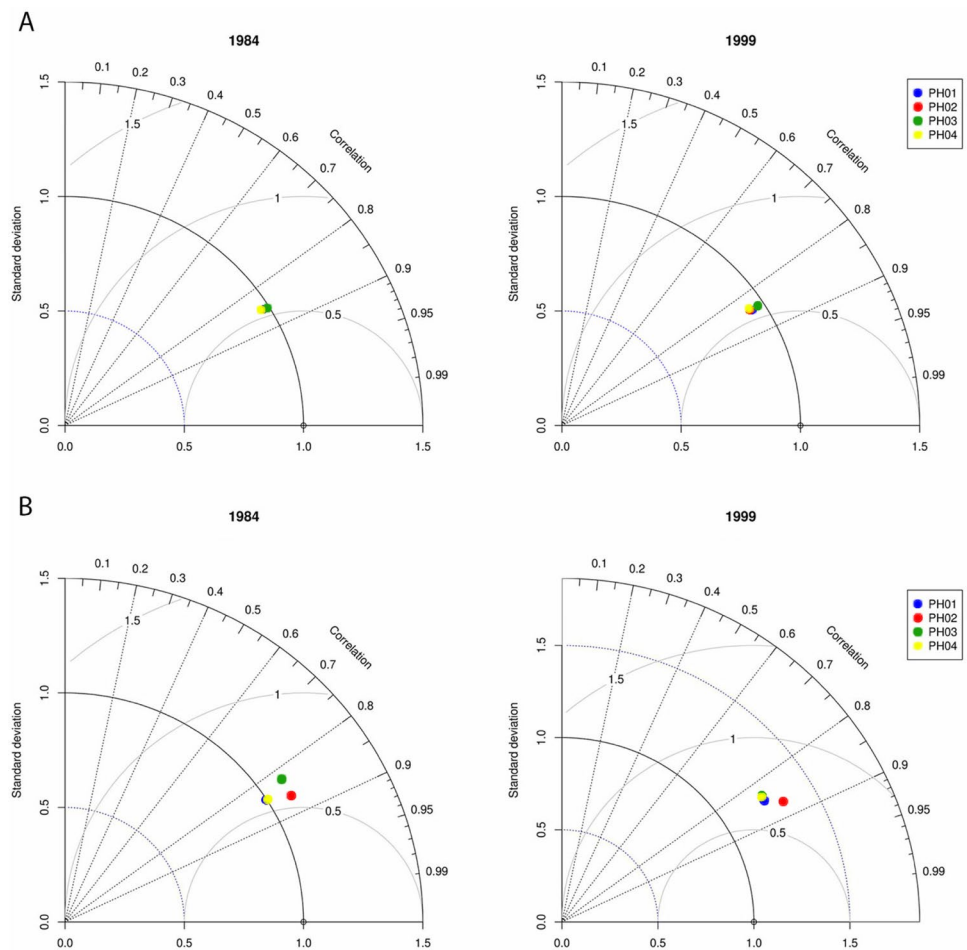


**Table 3** Comparison between Physics groups “1” and “4”

	Physics 1			Physics 4		
	RMSE	MAE	COR	RMSE	MAE	COR
Dry year (1984)	0.73	1.29	0.5	0.68	1.24	0.49
Wet year (1999)	1.0	1.15	0.47	0.96	1.09	0.5

We find that the WRF simulated precipitation, i.e. according to the distribution parameters, is underestimated by 30% compared to the observations, which is demonstrated in the Q–Q plot of Fig. 8a. The simulated precipitation is corrected by regressing the simulated precipitation against the observation, resulting in a multiplicative constant so that the fitted Weibull distribution of the WRF precipitation becomes 1.242 and 1.539 for the shape and scale factors, respectively. The Q–Q plot of the bias-corrected precipitation, shown in Fig. 8b, gives the best representation of the observations in the 30 years study period based on the probability distribution method.

The resulting bias-corrected precipitation is used as input for the SWAT hydrological model for the Gambella watershed for verification. The runoff results of the

hydrological model shown in Fig. 9a yield a very high coefficient of determination ( $R^2 = 0.88$ ), however, the runoff values were highly overestimated leading to a poor NSE ( $-0.15$ ), which is not acceptable for hydrological models. The bias-correction method based on the probability distribution is, therefore, rejected for hydrological applications, even though the statistical parameters indicate good agreement with observations.

The second correction method shows that bias is highly correlated to the terrain elevation, notably over the ETH, such that the bias-correction algorithm is a function of location and terrain elevation. The bias-correction matrices are divided into five bands based on elevation ranges, with band 1 representing the bias for grid points with elevation less than 500 m, band 2 from 500 to 1000 m, band 3 from 1000

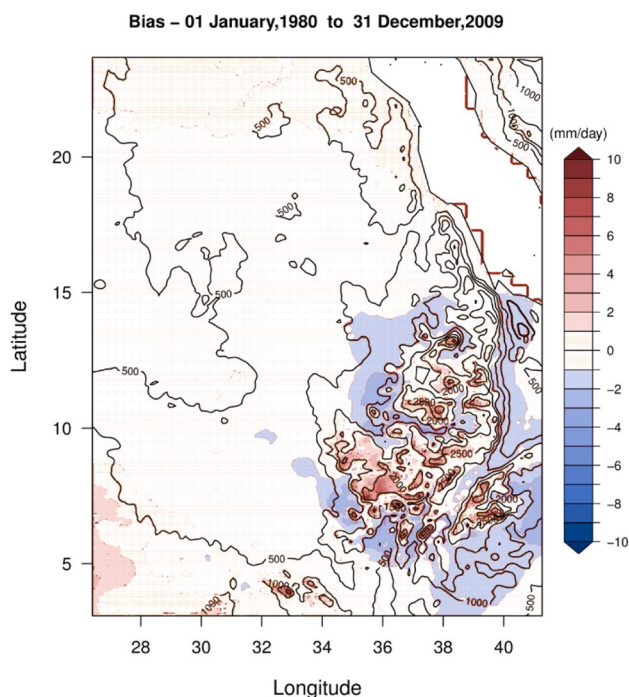


**Fig. 5** WRF modeled precipitation bias compared to GPCP showing the maximum bias over the Ethiopian highlands for the period 1980 to 2009. Solid black lines represent elevation contours

to 1500 m, band 4 from 1500 to 2000 m and band 5 for grids of altitude more than 2000 m as shown in Fig. 10.

The bias is corrected using the GPCP dataset and applied to the WRF model output at a condition that zero is the minimum value of precipitation. The resulting bias-corrected precipitation is again coupled with the SWAT hydrological model for the Gambella watershed. The runoff results of the hydrological model shown in Fig. 9b also yield a high coefficient of determination ( $R^2=0.80$ ) and a 0.61 NSE, which is considered sufficient for hydrological models.

In the third bias correction method, we generated 12 bias-correction matrices as daily average bias in each month (Fig. 11). It is clear that the bias in August is largest, with an underestimation of more than 10 mm/day, and smallest in May, July, and October, with almost no precipitation prediction bias.

The-bias corrected precipitation is similarly coupled to the SWAT model for the Gambella watershed to assess the correction method against the previous two methods. The runoff results of the hydrological model (Fig. 9c) yield a very high coefficient of determination ( $R^2=0.86$ ), and a very good NSE of 0.79, that is more reliable for hydrological models.

Hence, the three bias correction methods applied here resulted in statistically acceptable results (overall mean and standard deviation of the modeled precipitation), however, verification based on a hydrological model the results

for runoff were different. The spatiotemporal method was found to be the best bias-correction method, which should be applied to the modeled precipitation output for use in hydrologic applications.

## 4 Conclusions

Hydrological simulations, and quality of assessments based on their output, strongly depend on the input parameters, including precipitation. Due to the uncertainties and biases in modeling the temporal and spatial characteristics of precipitation, it is essential to reduce any biases before using it in such applications, for improving the overall process of decision making. The WRF model careful sensitivity analysis and optimization prior to model configuration domain (Abdelwares et al. 2017; Zittis et al. 2014, 2017), however, there are still biases in the produced output that require correction. The configured WRF model in this study shows a relatively high precision in simulating temperature with minor biases and errors based on the comparison with the observational datasets. However, the simulated precipitation is less accurate, and the results need to be bias-corrected to insure their validity for hydrologic applications.

The three bias-correction methods applied to WRF simulated precipitation output perform differently when compared to the rainfall-runoff hydrological model results. The spatiotemporal method, assuming a repeating monthly bias cycle throughout the years over the period considered appears to yield optimal performance, producing a valid precipitation product for the EN region at a high resolution, appropriate for hydrologic applications. The spatiotemporal method improved the NSE value of the runoff results using the WRF corrected precipitation from  $-0.15$  for the probability distribution correction method to 0.79, as well as preserving the high  $R$ -squared value at around 0.86.

Hydrological verification of the bias-correction method is found to be an essential step in approving the correction method since the results need to be used in hydrologic applications. Further, our results with the WRF model give confidence that scenario calculations will be useful for the future projection of temperature and precipitation, the latter at the condition of considering bias-correction with the proposed algorithm (Spatiotemporal Method). The success of this method also underscores the weakness of climate models in reproducing rainfall in regions with pronounced topography. It is worth noting that the suggested bias-correction methods are subject to the study region and may show different performance if applied to other climatic and topographic regions.

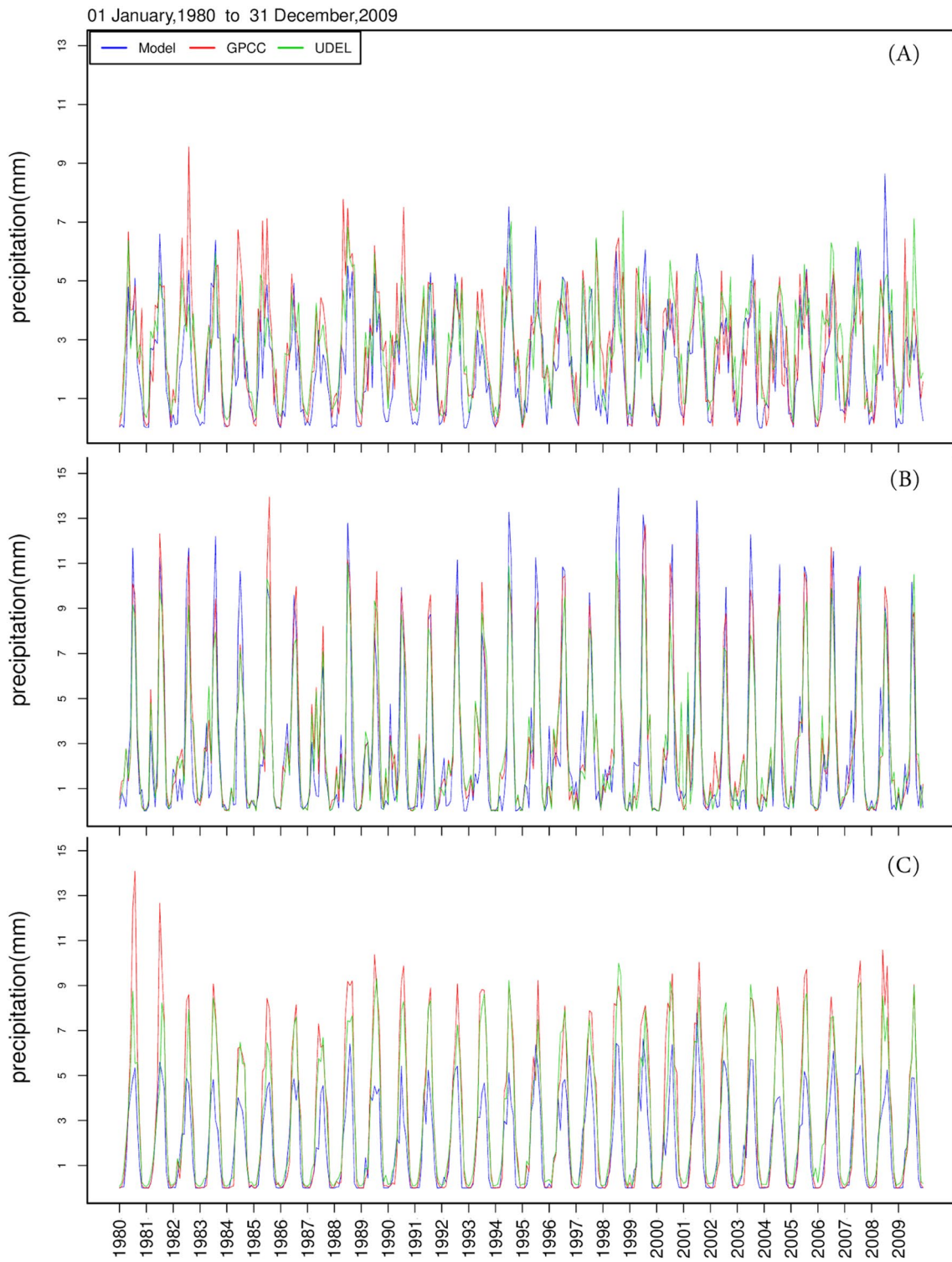
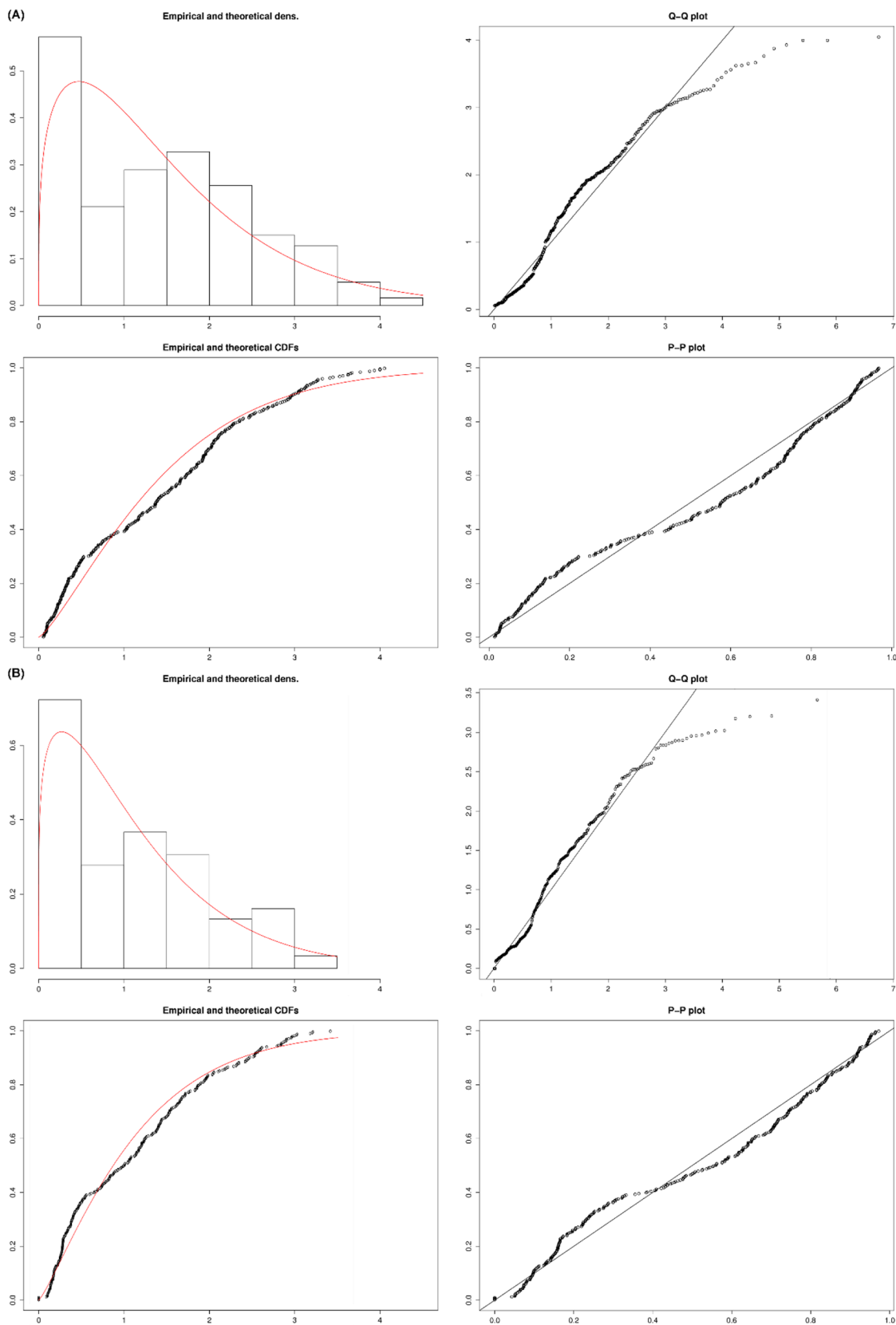
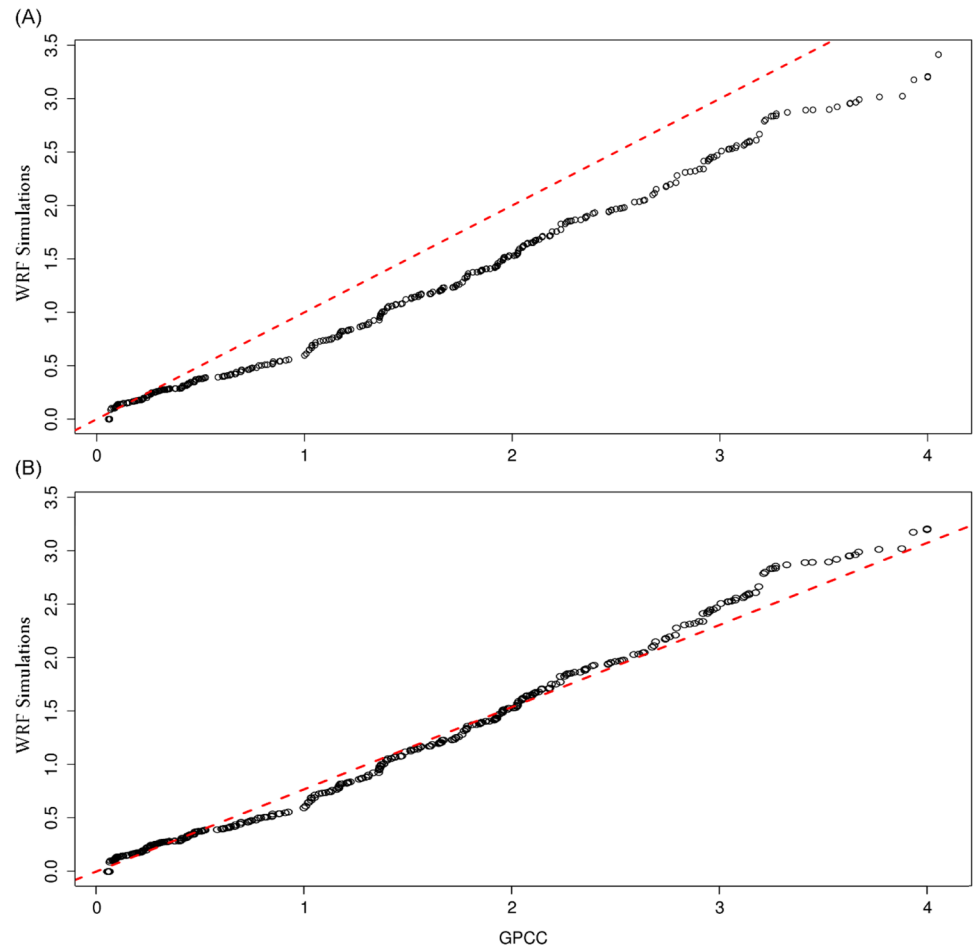


Fig. 6 WRF modeled precipitation time series at: **a** Akobo, **b** BN and **c** GERD



**Fig. 7** a GPCP precipitation Weibull distribution fitting. b WRF precipitation Weibull distribution fitting

**Fig. 8** **a** Q–Q plot for the modeled precipitation vs. the GPCC data. **b** Q–Q plot for the bias-corrected simulated precipitation vs. the GPCC data



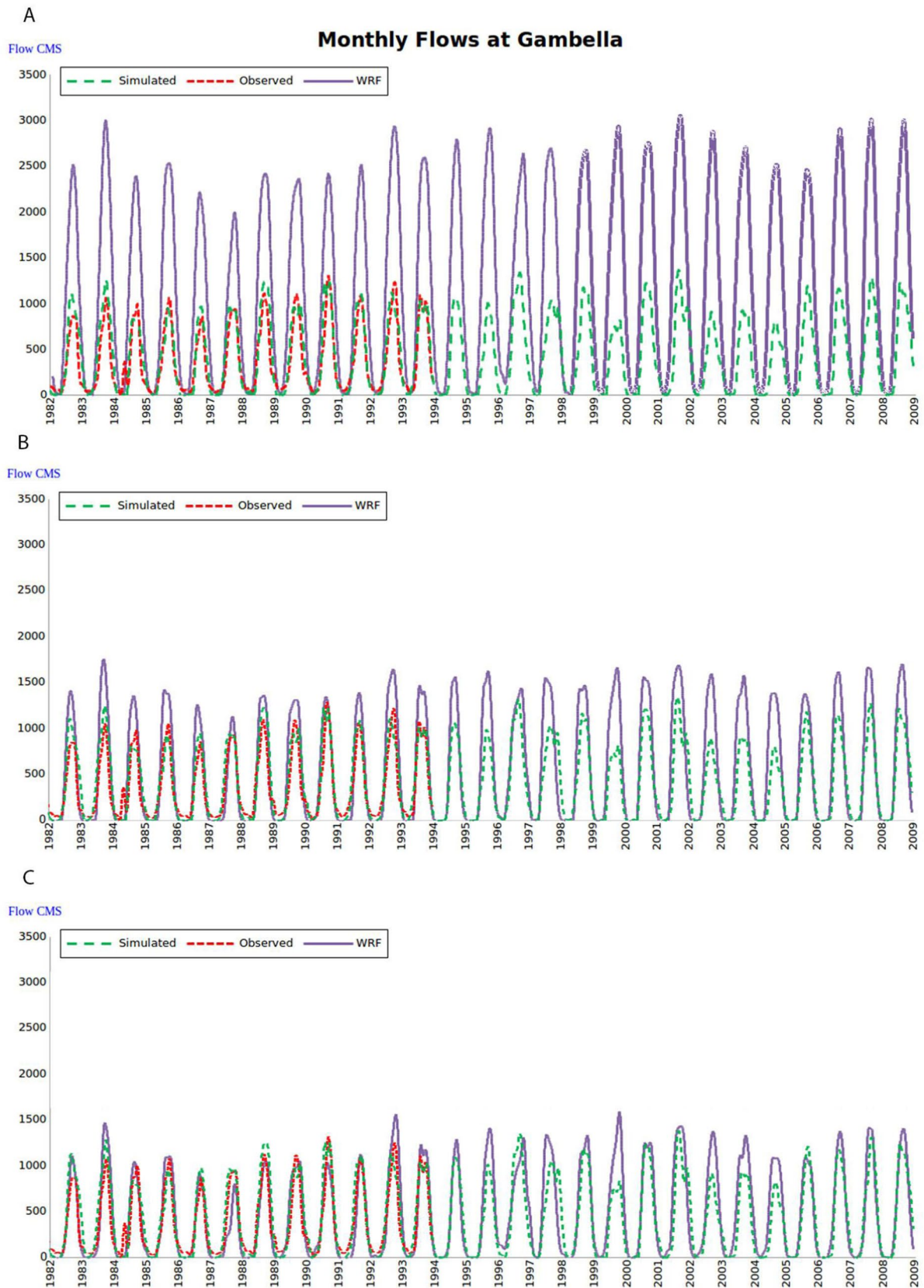


**Fig. 9** Comparison of monthly flow at Gambella watershed between the calibrated SWAT hydrological model forced by ground observations and WRF bias-corrected precipitation: **a** probability distribution corrected, **b** elevation-location corrected, **c** spatiotemporal corrected

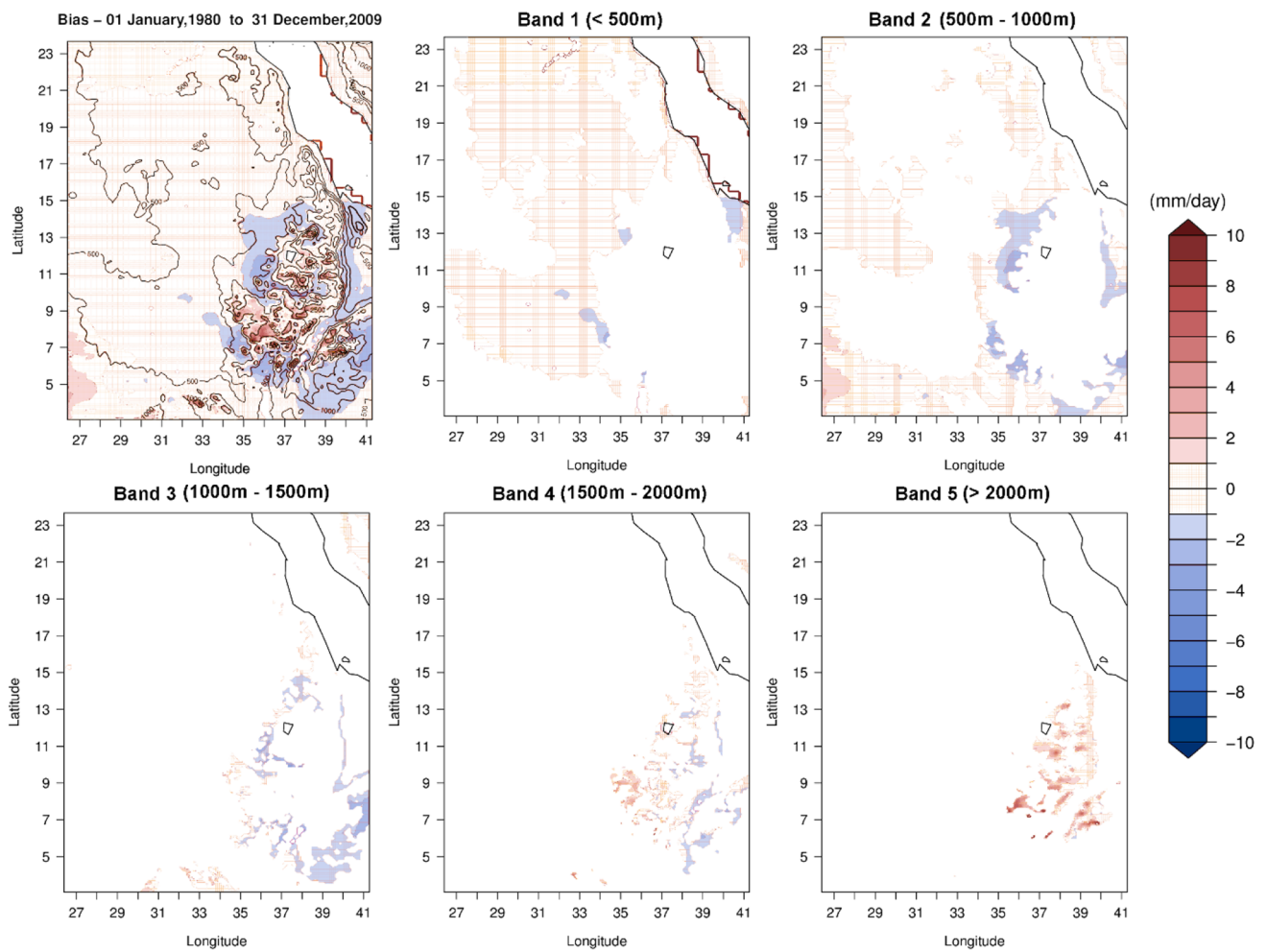


**Fig. 10** (Left) WRF 30-year mean precipitation bias and terrain elevation contour lines. (Right) The decomposed precipitation bias in the five elevation bands

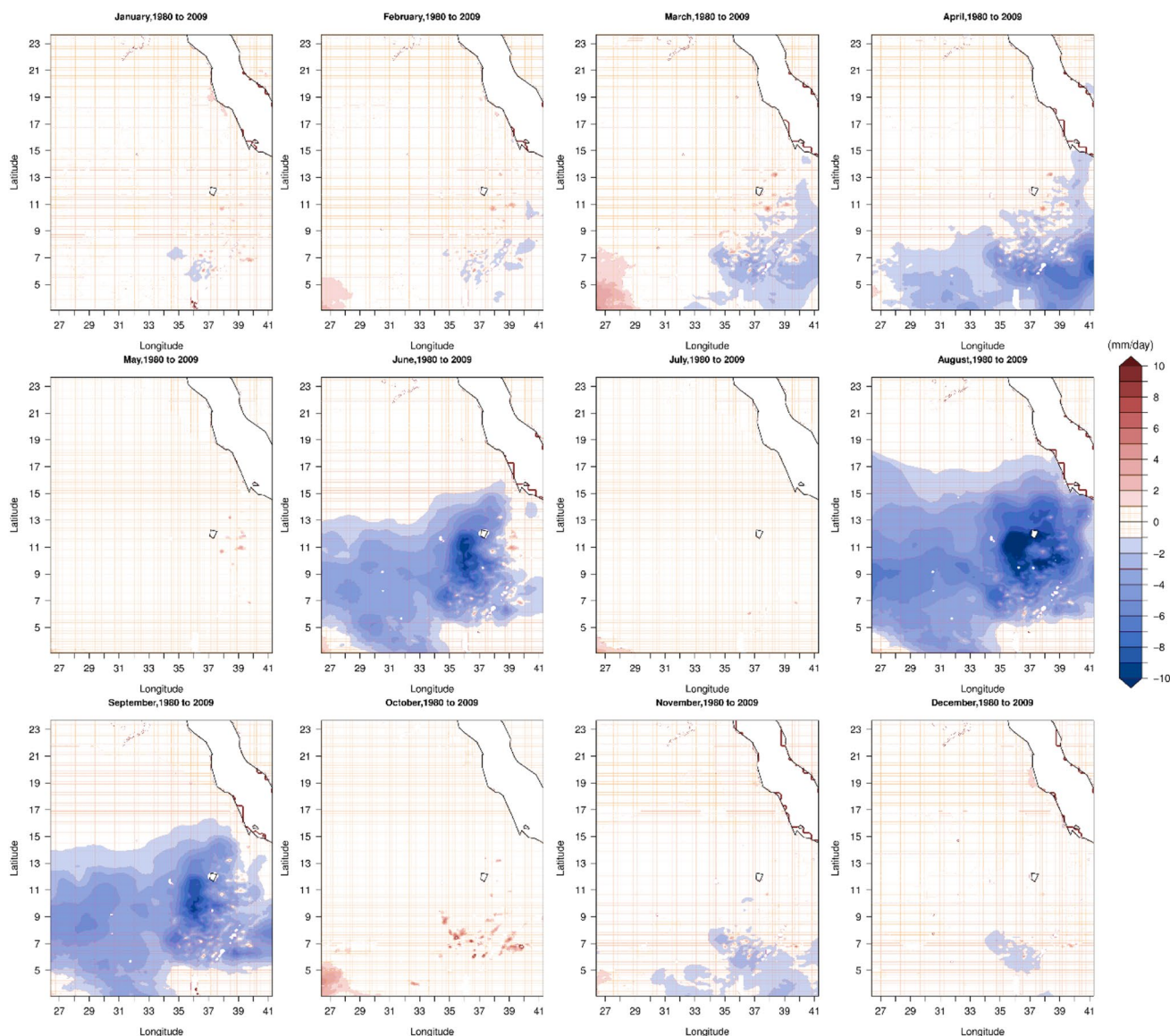


**Fig. 11** Monthly spatiotemporal precipitation bias corrections

**Acknowledgements** Sincere acknowledgements are due to Cairo University, The Cyprus Institute and Max Plank Institute for Chemistry. Special acknowledgement is due to CORDEX for support through training, computational resources and the professional technical assistance.

**Data Availability** All datasets used in this study are cited in references.

**Code Availability** Dynamic downscaling is performed using the open-source WRF model and all data analysis is carried out using the open-source R programming language.

## Declarations

**Conflict of Interest** The authors declare that they have no conflict of interest.

## References

- Abdelwares M, Haggag M, Wagdy A, Lelieveld J (2017) Customized framework of the WRF model for regional climate simulation over the eastern NILE basin. *Theor Appl Climatol* 134(3–4):1135–1151. <https://doi.org/10.1007/s00704-017-2331-2>

- Almazroui M, Saeed F, Saeed S, Nazrul Islam M, Ismail M, Klutse NAB, Siddiqui MH (2020) Projected change in temperature and precipitation over Africa from CMIP6. *Earth Syst Environ* 4:455–475. <https://doi.org/10.1007/s41748-020-00161-x>
- Argent RE (2014) Customization of the WRF model over the lake Victoria Basin in East Africa. North Carolina State University
- Argüeso D, Evans JP, Fita L (2013) Precipitation bias correction of very high resolution regional climate models. *Hydrol Earth Syst Sci* 17(11):4379–4388. <https://doi.org/10.5194/hess-17-4379-2013>
- Arnold JG, Fohrer N (2005) Swat 2000: current capabilities and research opportunities in applied watershed modelling. *Hydrol Process* 19(3):563–572. <https://doi.org/10.1002/hyp.5611>
- Asore (2012) Impact of climate change on potential evapotranspiration and runoff in the Awash River basin in Ethiopia. MSc Thesis. Cairo University. Egypt.
- Baumberger C, Knutti R, Hirsch Hadorn G (2017) Building confidence in climate model projections: an analysis of inferences from fit. *Wiley Interdiscip Rev Clim Change*. <https://doi.org/10.1002/wcc.454>
- Berrisford P, Dee DP, Poli P, Brugge R, Fielding K, Fuentes M, Simmons A (2011). The ERA-Interim archive Version 2.0. ERA Report Series. Shinfield Park, Reading: ECMWF.
- Beysene T, Lettenmaier DP, Kabat P (2010) Hydrologic impacts of climate change on the Nile River Basin: implications of the 2007 IPCC scenarios. *Clim Change* 100(3–4):433–461. <https://doi.org/10.1007/s10584-009-9693-0>
- Buontempo C, Mathison C, Jones R, Williams K, Wang C, McSweeney C (2015) An ensemble climate projection for Africa. *Clim Dyn* 44(7–8):2097–2118. <https://doi.org/10.1007/s00382-014-2286-2>
- Caldwell P, Chin HNS, Bader DC, Bala G (2009) Evaluation of a WRF dynamical downscaling simulation over California. *Clim Change* 95(3–4):499–521. <https://doi.org/10.1007/s10584-009-9583-5>
- Camera C, Bruggeman A, Zittis G, Sofokleous I, Arnault J (2020) Simulation of extreme rainfall and streamflow events in small Mediterranean watersheds with a one-way coupled atmospheric-hydrologic modelling system. *Nat Hazards Earth Syst Sci Discuss*. <https://doi.org/10.5194/nhess-2020-43>
- Chen S-H, Sun W-Y (2002) A one-dimensional time dependent cloud model. *J Meteorol Soc Jpn* 80(1):99–118. <https://doi.org/10.2151/jmsj.80.99>
- Chen F, Mitchell K, Schaake J, Xue Y, Pan H-L, Koren V, Betts A (1996) Modeling of land surface evaporation by four schemes and comparison with FIFE observations. *J Geophys Res* 101(D3):7251. <https://doi.org/10.1029/95JD02165>
- Clarke, L. E., Jacoby, H., Pitcher, H., Reilly, J., & Richels, R. (2007). Scenarios of Greenhouse Gas Emissions and Atmospheric, (July), 154.
- Cohen SJ (1990) Bringing the global warming issue closer to home: the challenge of regional impact studies. *Bull Am Meteor Soc*. [https://doi.org/10.1175/1520-0477\(1990\)071%3c0520:BTG-WIC%3e2.0.CO;2](https://doi.org/10.1175/1520-0477(1990)071%3c0520:BTG-WIC%3e2.0.CO;2)
- Collins WD, Rasch PJ, Boville BA, Hack JJ, McCaa JR, Williamson DL, Zhang M (2006) The formulation and atmospheric simulation of the Community Atmosphere Model version 3 (CAM3). *J Clim* 19(11):2144–2161. <https://doi.org/10.1175/JCLI3760.1>
- Collins M, Knutti R, Arblaster J, Dufresne J-L, Fichefet T, Friedlingstein P, Gao X, Gutowski WJ, Johns T, Krinner G, Shongwe M, Tebaldi C, Weaver AJ, Wehner MF, Allen MR, Andrews T, Beyerle U, Bitz CM, Bony S, Booth BBB (2013) Long-term climate change: projections, commitments and irreversibility. In: Stocker TF, Qin D, Plattner G-K, Tignor MMB, Allen SK, Boschung J, Nauels A, Xia Y, Bex V, Midgley PM (eds) *Climate change 2013 - The physical science basis: Contribution of Working Group I to the fifth assessment report of the Intergovernmental Panel on Climate Change (Intergovernmental Panel on Climate Change)*. Cambridge University Press, pp 1029–1136
- Di Baldassarre G, Elshamy M, van Griensven A, Soliman E, Kigobe M, Ndomba P, Uhlenbrook S (2011) Future hydrology and climate in the River Nile basin: a review. *Hydrol Sci J* 56(2):199–211. <https://doi.org/10.1080/02626667.2011.557378>
- Done JM, Leung LR, Davis CA, Kuo B (2005) Regional Climate Simulation Using the WRF Model. In WRF/MM5 User's Workshop.
- Driouech F, ElRhazi K, Moufouma-Okia W, Arjald K, Balhane S (2020) Assessing future changes of climate extreme events in the CORDEX-MENA region using regional climate model ALADIN-climate. *Earth Syst Environ* 4:477–492. <https://doi.org/10.1007/s41748-020-00169-3>
- Elshamy ME, Seierstad IA, Sorteberg A (2009) Impacts of climate change on Blue Nile flows using bias-corrected GCM scenarios. *Hydrol Earth Syst Sci* 13(5):551–565. <https://doi.org/10.5194/hess-13-551-2009>
- ENTRO (2006) Water Atlas of the Blue Nile Sub-Basin. Eastern Nile Technical Regional Office technical report. Available at: <https://entrospace.nilebasin.org/handle/20.500.12351/31>.
- Evans JP (2012) Regional Climate Modelling: The Future for Climate Change Impacts and Adaptation Research. Retrieved April 5, 2016, from <http://www.earthzine.org/2012/02/14/regional-climate-modelling-the-future-for-climate-change-impacts-and-adaptation-research/>
- Fujino J, Nair R, Kainuma M, Masui T, Matsuoka Y (2006) Multi-gas Mitigation Analysis on Stabilization Scenarios Using Aim Global Model. *The Energy Journal*, 27, 343–353. Retrieved from <http://www.jstor.org/stable/23297089>
- Gbobaniyi E, Sarr A, Sylla MB, Diallo I, Lennard C, Dosio A, Lamptey B (2014) Climatology, annual cycle and interannual variability of precipitation and temperature in CORDEX simulations over West Africa. *Int J Climatol* 34(7):2241–2257. <https://doi.org/10.1002/joc.3834>
- Giorgi F (1990) Simulation of regional climate using a limited area model nested in a general circulation model. *J Clim* 3(9):941–963. [https://doi.org/10.1175/1520-0442\(1990\)003%3c0941:SORCUA%3e2.0.CO;2](https://doi.org/10.1175/1520-0442(1990)003%3c0941:SORCUA%3e2.0.CO;2)
- Janjić ZI (1990) The step-mountain coordinate: physical package. *Mon Weather Rev* 118(7):1429–1443. [https://doi.org/10.1175/1520-0493\(1990\)118%3c1429:TSMCPP%3e2.0.CO;2](https://doi.org/10.1175/1520-0493(1990)118%3c1429:TSMCPP%3e2.0.CO;2)
- Janjić ZI (1994) The step-mountain eta coordinate model: further developments of the convection, viscous sublayer, and turbulence closure schemes. *Mon Weather Rev* 122(5):927–945. [https://doi.org/10.1175/1520-0493\(1994\)122%3c0927:TSMCEM%3e2.0.CO;2](https://doi.org/10.1175/1520-0493(1994)122%3c0927:TSMCEM%3e2.0.CO;2)
- Jin J, Miller NL, Schlegel N (2010) Sensitivity study of four land surface schemes in the WRF model. *Adv Meteorol* 2010(November):1–11. <https://doi.org/10.1155/2010/167436>
- Kalognomou E-A, Lennard C, Shongwe M, Pinto I, Favre A, Kent M, Büchner M (2013) A diagnostic evaluation of precipitation in CORDEX models over Southern Africa. *J Clim* 26(23):9477–9506. <https://doi.org/10.1175/JCLI-D-12-00703.1>
- Katragkou E, García-Díez M, Vautard R, Sobolowski S, Zanits P, Alexandri G, Jacob D (2015) Regional climate hindcast simulations within EURO-CORDEX: evaluation of a WRF multi-physics ensemble. *Geosci Model Dev* 8(3):603–618. <https://doi.org/10.5194/gmd-8-603-2015>
- Laprise R, Hernández-Díaz L, Tete K, Sushama L, Šeparović L, Martynov A, Valin M (2013) Climate projections over CORDEX Africa domain using the fifth-generation Canadian regional climate model (CRCM5). *Clim Dyn* 41(11–12):3219–3246. <https://doi.org/10.1007/s00382-012-1651-2>
- Legates DR, McCabe GJ (1999) Evaluating the use of “goodness-of-fit” measures in hydrologic and hydroclimatic model validation.

- Water Resour Res 35(1):233–241. <https://doi.org/10.1029/1998WR900018>
- Lelieveld J, Hadjinicolaou P, Kostopoulou E, Chenoweth J, Maayar M, Giannakopoulos C, Xoplaki E (2012) Climate change and impacts in the Eastern Mediterranean and the Middle East. *Clim Change* 114(3):667–687. <https://doi.org/10.1007/s10584-012-0418-4>
- Lelieveld J, Proestos Y, Hadjinicolaou P, Tanarhte M, Tyrllis E, Zittis G (2016) Strongly increasing heat extremes in the Middle East and North Africa (MENA) in the 21st century. *Clim Change* 137:245–260. <https://doi.org/10.1007/s10584-016-1665-6>
- Mengistu DT, Sorteberg A (2012) Sensitivity of SWAT simulated streamflow to climatic changes within the Eastern Nile River basin. *Hydrol Earth Syst Sci* 16(2):391–407. <https://doi.org/10.5194/hess-16-391-2012>
- Mohamed YA, van den Hurk BJJM, Savenije HHG, Bastiaanssen WGM (2005) Hydroclimatology of the Nile: results from a regional climate model. *Hydrol Earth Syst Sci* 9(3):263–278. <https://doi.org/10.5194/hess-9-263-2005>
- Nicholson SE, Some B, McCollum J, Nelkin E, Klotter D, Berte Y, Diallo BM, Gaye I, Kpabeba G, Ndiaye O, Noukpozoukou JN, Tanu MM, Thiam A, Toure AA, Traore AK (2003) Validation of TRMM and other rainfall estimates with a high-density gauge dataset for West Africa Part i: validation of GPCP rainfall product and Pre-TRMM satellite and blended products. *J Appl Meteorol* 42(10):1337–1354
- Otkin JA, H-L Huang, A Seifert (2006) A comparison of microphysical schemes in the WRF model during a severe weather event. In 7th Annual WRF User's Workshop. Boulder, CO, NCAR.
- Raafat A (2015) Assessment of the Impacts of Proposed Water Resources Development Projects in Baro-Akobo-Sobat Basin on HAD. MSc Thesis. Cairo University.
- Schamm K, Ziese M, Becker A, Finger P, Meyer-Christoffer A, Schneider U, Stender P (2014) Global gridded precipitation over land: a description of the new GPCP first guess daily product. *Earth Syst Sci Data* 6(1):49–60. <https://doi.org/10.5194/essd-6-49-2014>
- Schmidli J, Goodess CM, Frei C, Haylock MR, Hundscha Y, Ribalaygua J, Schmith T (2007) Statistical and dynamical downscaling of precipitation: an evaluation and comparison of scenarios for the European Alps. *J Geophys Res* 112:D04105. <https://doi.org/10.1029/2005JD007026>
- Shin HH, Hong S-Y (2011) Intercomparison of planetary boundary-layer parametrizations in the WRF model for a single day from CASES-99. *Bound-Layer Meteorol* 139(2):261–281. <https://doi.org/10.1007/s10546-010-9583-z>
- Siam M (2010) Impact of Climate Change on the Upper Blue Nile Catchment Flows Using IPCC Scenarios. MSc Thesis. Cairo University.
- Skamarock WC, Klemp JB, Dudhia J, Gill DO, Barker D, Duda MG, Huang X, Wang W, Powers JG (2008) A Description of the advanced research WRF version 3 (No. NCAR/TN-475+STR). University Corporation for Atmospheric Research. <https://doi.org/10.5065/D68S4MVH>
- Soares PMM, Cardoso RM, Miranda PMA, Medeiros J, Belo-Pereira M, Espirito-Santo F (2012) WRF high resolution dynamical downscaling of ERA-Interim for Portugal. *Clim Dyn* 39(9):2497–2522. <https://doi.org/10.1007/s00382-012-1315-2>
- Tanarhte M, Hadjinicolaou P, Lelieveld J (2012) Intercomparison of temperature and precipitation data sets based on observations in the Mediterranean and the Middle East. *J Geophys Res Atmos*. <https://doi.org/10.1029/2011JD017293>
- Tarabia A (2015) Impact Assessment of the Proposed Water Resources Development Projects in the Blue Nile Basin on Nile Flow at Aswan. MSc Thesis. Cairo University.
- Tesemma Z (2009) Long Term Hydrologic Trends in the Nile Basin. MSc Thesis. Cornell University.
- UDeI. (2015). UDeI\_AirT\_Precip data. Boulder, CO: NOAA/OAR/ESRL PSD. Retrieved from <http://www.esrl.noaa.gov/psd/>
- Weldemariam HG (2015) Dynamical downscaling of GCM outputs to determine impacts of climate change and variability on the hydrologic sensitivity of Blue Nile Basin surface water resource potential. University of Nebraska
- Zittis G (2018) Observed rainfall trends and precipitation uncertainty in the vicinity of the Mediterranean, Middle East and North Africa. *Theor Appl Climatol* 134:1207–1230. <https://doi.org/10.1007/s00704-017-2333-0>
- Zittis G, Bruggeman A, Camera C, Hadjinicolaou P, Lelieveld J (2017) The added value of convection permitting simulations of extreme precipitation events over the eastern Mediterranean. *Atmos Res* 191:20–33. <https://doi.org/10.1016/j.atmosres.2017.03.002>
- Zittis G, Hadjinicolaou P, Klangidou M, Proestos Y, Lelieveld J (2019) A multi-model, multi-scenario, and multi-domain analysis of regional climate projections for the Mediterranean. *Reg Environ Change* 19(8):2621–2635. <https://doi.org/10.1007/s10113-019-01565-w>
- Zittis G, Hadjinicolaou P, Lelieveld J (2014) Comparison of WRF model physics parameterizations over the MENA-CORDEX domain. *Am J Clim Chang* 3(5):490–511. <https://doi.org/10.4236/ajcc.2014.35042>